Chapter 3

The effect of dust particles on the evolution of weak discontinuity in two-dimensional supersonic flow of van der Waals gas *

"The essence of mathematics lies in its freedom."

–Georg Cantor

3.1 Introduction

In this chapter, we consider the system describing 2-D van der Waals dusty gas flow which is nothing but a composition of a van der Waals gas and solid dust particles.

* "The contents of this chapter have been published in ***Eur. Phys. J. Plus (2022) 137:223.***"

This composition does not contain the volume of the solid particle more than 5% of the total volume of the mixture. The study of non-linear waves in van der Waals dusty gas flow have significant role due to its applications to volcanic and cosmic explosions, coal mines blast, underground, metalized propellant, supersonic flight in polluted air, nozzle flow, lunar ash flow and many engineering science problems (See [109], [110], [10], [111], [112], [113]). Also, in many astrophysical phenomena, the composition of dust particles and gases play crucial role. Miura [111, 10] have examined the wave propagation and its behavior through dusty gas layer. Also, he described the condition for the separation of pure gas from a mixture of gas with dust particles. The author [110] has investigated the problem of blast waves in a dusty medium and discussed that as to how the decay of blast waves is affected in dusty gas. In recent, the authors in [113], [114], [115], [116], [83, 92] have studied the solution of the shock propagation in dusty gas by several approaches. Mehla et al. [117] have further discussed the wave propagation in relaxing gases with solid particles. The dusty gas flow has also drawn the focus of the many authors due to its advantages in industrial and environmental fields.

In this theoretical work, we study about the formation of shock wave in 2-D steady supersonic flow of the composition of van der Waals gas and small solid dust particles for planar and non-planar cases by using method of wavefront analysis. This method is very useful to examine the occurrence of shock wave and shock formation distance in 2-D gas dynamic flow. Also, the impact of the upstream flow Mach number in the presence of van der Waals gas and dust particles on the shock formation distance is discussed. A concise explanation of the method of wavefront analysis is discussed by [78], [75], [67], and [79]. [80] have discussed the shock formation distance in 2-D radiative magnetogasdynamic flow over a concave corner. [81] has examined the evolution of the shock wave and obtained the relation for shock formation distance

in 2-D radiating gas flow and radiative van der Waals gas flow by using same technique. Furthermore, the author [83] has also studied the shock formation distance phenomena in 2-D dusty gas.

In all of the above literature, the study of shock formation and variation in shock formation distance in 2-D steady supersonic flow of the composition of van der Waals gas and dust particles by using the method of wavefront analysis have not been discussed by any researcher. The goal of this study is to discuss the conditions of the occurrence of shock wave and derive the relation for shock formation distance for planar, cylindrically symmetric and spherically symmetric flows of the mixture of van der Waals gas and small solid dust particles. Also, we show the impact of van der Waals gas parameter and dust particles on the shock formation distance. The investigation of shock wave in van der Waals gas flow have great consideration of engineers and scientists due to its important role in the study of several areas like atmospheric science, oceanography, astrophysics, hypervelocity impact, hypersonic flow and aerodynamics. Many interesting results of the shock wave in van der Waals gas have been considered in recent years by many researchers as in [93], [94], [95], [96],[87], [118] and [84]. But study of the problem of the weak discontinuity in van der Waals gas in dusty gas is more typical problem in theoretical investigation. Recently, we have seen that the propagation of shock wave and its evolutionary behavior for planar and non-planar van der Waals gas dynamic flow in the presence of solid particles is also studied in [119], [115], [116], [91] and [120].

Present chapter is structured into the following sections as: in section (3.2), we consider the governing equations describing the two-dimensional supersonic van der Waals gas flow with dust particles. It also contains the characteristic formulation of governing equations. Section (3.3) contains the derivation of the transport equations for the discontinuity wave by introducing new curvilinear co-ordinates. Further, in

section (3.4), the steepening of shock wave with the help of transport equations obtained in section (3.3) is discussed. We have analyzed the results of this study for "planar, cylindrically symmetric and spherically symmetric cases" in section (3.5). Section (3.6) contains the conclusions of this study.

3.2 Governing equations and its characteristic formulation

The governing equations describing 2-D steady supersonic flow of van der Waals gas with dust particles may be written as [93, 83]

$$u\rho_x + v\rho_y + \rho u_x + \rho v_y + \rho n v y^{-1} = 0, \tag{3.1}$$

$$\rho u u_x + \rho v u_y + p_x = 0, \tag{3.2}$$

$$\rho u v_x + \rho v v_y + p_y = 0, \tag{3.3}$$

$$up_x + vp_y - C^2\left(u\rho_x + v\rho_y\right) = 0, \tag{3.4}$$

where p, ρ are the pressure, gas density and u, v are the components of velocity along the x and y- axes, respectively. The parameter n is a constant, where the value $n = 0$ is used for planar flow and the value $n = 1, 2$ is used for non-planar flow. The parameter C represents the speed of sound in van der Waals gas with dust particles defined as

$$C^2 = \frac{(\Gamma - \omega_2\rho^2)p}{(1 - \omega_1\rho + \omega_2\rho^2)\rho},$$

where $\omega_1 = \theta + \tilde{b}$ and $\omega_2 = \theta\tilde{b}$, and $\tilde{b}$ is van der Waals excluded volume. The

Grüneisen coefficient Γ is defined by

$$\Gamma = \frac{\gamma(1+\lambda\beta)}{(1+\lambda\beta\gamma)},$$

where $Z = V_{sp}/V_g$, with V_g as the total volume of the mixture and V_{sp} is the volumetric extension of the solid particles, $\beta = c_{sp}/c_p$, $\lambda = k_p/(1-k_p)$ and $\gamma = c_p/c_v$. Here, k_p is the mass fraction of dust particles that is $k_p = m_{sp}/m_g$, where m_{sp} is the mass of the dust particles and m_g is the total mass of the mixture. The parameters c_{sp}, c_p and c_v are known as the specific heat of solid particles, the specific heat of the gas at constant pressure and at constant volume, respectively. The mass fraction k_p and volume fraction Z are related by $Z = \theta\varrho$, $\theta = k_p/\varrho_{sp}$, where ϱ_{sp} is the specific density of the dust particles. The equation of state of the mixture of the van der Waals gas and small solid particles is given as

$$p = \frac{(1-k_p)}{(1-Z)(1-\tilde{b}\rho)}\rho\Re T, \tag{3.5}$$

where $\Re$ and T are the gas constant and temperature, respectively.

The following cases arise, depending on the values of the parameters θ and b.

Case 1: When $\theta = 0$ and $b \neq 0$, then Γ becomes γ, $C^2 = \frac{\gamma p}{(1-\tilde{b}\rho)\rho}$ that is the flow becomes van der Waals gas flow in a dust free medium.

Case 2: When $\theta = 0$ and $b = 0$, then Γ becomes γ, $C^2 = \frac{\gamma p}{\rho}$, and the mixture becomes ideal in the absence of dust particles.

Case 3: When $\theta \neq 0$ and $b = 0$, in this case $\Gamma \neq 0$, $C^2 = \frac{\Gamma p}{(1-Z)\rho}$, and the flow becomes ideal gas flow with dust particles.

Case 4: When $\theta \neq 0$ and $b \neq 0$, in this case $\Gamma \neq 0$, $C^2 = \frac{(\Gamma-\omega_2\rho^2)p}{(1-\omega_1\rho+\omega_2\rho^2)\rho}$, and the flow becomes van der Waals gas flow with dust particles.

The governing equation (3.1) − (3.5) can be written in a matrix form as

$$W_t + A(W)W_x + B = 0, \tag{3.6}$$

where A is the matrix of order 4×4 and W, B are column matrices which are given by,

$$W = \begin{bmatrix} \rho \\ u \\ v \\ p \end{bmatrix}, A(W) = \frac{1}{(u^2-C^2)} \begin{bmatrix} \frac{v\left(u^2-C^2\right)}{u} & -\rho v & \rho u & \frac{v}{u} \\ 0 & uv & -C^2 & \frac{-v}{\rho} \\ 0 & 0 & \frac{v\left(u^2-C^2\right)}{u} & \frac{\left(u^2-C^2\right)}{\rho u} \\ 0 & -C^2\rho v & C^2\rho u & uv \end{bmatrix} \text{ and } B = \frac{1}{(u^2-C^2)} \begin{bmatrix} \frac{nvu}{y} \\ \frac{-C^2nv}{y} \\ 0 \\ \frac{C^2\rho nvu}{y} \end{bmatrix}.$$

The eigenvalues of matrix $A(W)$ are represented by $\lambda^{(i)}$ for $i = 1, 2, 3, 4$, obtained as

$$\lambda^{(1)} = \frac{v}{u}, \quad \lambda^{(2)} = \frac{v}{u}, \quad \lambda^{(3)} = \frac{uv + C^2\left(M^2-1\right)^{1/2}}{u^2-C^2}, \quad \lambda^{(4)} = \frac{uv - C^2\left(M^2-1\right)^{1/2}}{u^2-C^2}, \tag{3.7}$$

and the left eigenvectors corresponding to these eigenvalues are

$$\begin{aligned} L^{(1)} &= \begin{pmatrix} 0 & 1 & \frac{v}{u} & \frac{1}{\rho u} \end{pmatrix}, \quad L^{(2)} = \begin{pmatrix} 1 & 0 & 0 & -\frac{1}{C^2} \end{pmatrix}, \\ L^{(3)} &= \begin{pmatrix} 0 & 1 & -\frac{u}{v} & \frac{-\left(M^2-1\right)^{1/2}}{\rho v} \end{pmatrix}, \quad L^{(4)} = \begin{pmatrix} 0 & 1 & -\frac{u}{v} & \frac{\left(M^2-1\right)^{1/2}}{\rho v} \end{pmatrix}, \end{aligned} \tag{3.8}$$

where M is the upstream flow Mach number defined as $M^2 = \frac{q^2}{C^2}$, with $q^2 = u^2 + v^2$. From (3.7) and (3.8), it is clear that the system (3.6) has four real eigenvalues and four linearly independent left eigenvectors corresponding to these which is sufficient to show that system (3.6) is hyperbolic in nature and have two characteristics curves along $dy/dx = \lambda^{(3,4)}$. These two curves propagate along the characteristic curve $\frac{dy}{dx} = \lambda^{(3,4)}$ in opposite directions with speeds $\lambda^{(3,4)}$, respectively.

3.3 Transport equations for the evolution of weak discontinuity

In this section, the transport equations which lead to investigate the formation of weak discontinuity in van der Waals dusty gas, will be derived by employing the method of wavefront analysis. Assuming $\lambda^{(3)}$ which represents the initial wavefront $\zeta(x,y)=0$, goes through the point (x_0,y_0), and the medium ahead of this $\zeta(x,y)=0$, have uniform pressure p_0, uniform density ρ_0, uniform velocity u_0 in x-direction with $v_0=0$ and uniform temperature $T_0=T_b$, where "the suffix-0 shows the quantity defined in the region ahead of $\zeta(x,y)=0$".

On introducing a new curvilinear co-ordinates ζ, y' which are given by (See [83])

$$\zeta_x+\lambda^{(3)}\zeta_y=0, \tag{3.9}$$

$$\zeta(x,y_0)=x-x_0, \tag{3.10}$$

and $y=y'$. Here ζ is positive behind of the leading characteristic curve on which $\zeta(x,y)=0$ and ζ is negative ahead of the leading characteristic curve on which $\zeta(x,y)=0$. In the new curvilinear co-ordinates, pre-multiplying by $L^{(j)}$, we have following form

$$\begin{aligned}
& L^{(j)}W_x+L^{(j)}A(W)W_y+L^{(j)}B=0,\\
\text{or}\quad & L^{(j)}W_\zeta\zeta_x+L^{(j)}A(W)\left(W_\zeta\left(-\frac{\zeta_x}{\lambda^3}\right)+W_{y'}\right)+L^{(j)}B=0,\\
\text{or}\quad & L^{(j)}W_\zeta+\frac{\lambda^{(j)}\lambda^{(3)}}{\lambda^{(3)}-\lambda^{(j)}}\frac{1}{\zeta_x}L^{(j)}W_{y'}+\frac{\lambda^{(3)}}{\lambda^{(3)}-\lambda^{(j)}}\frac{1}{\zeta_x}L^{(j)}B=0,\\
\text{or}\quad & \left(\lambda^{(3)}-\lambda^{(j)}\right)L^{(j)}W_\zeta+\lambda^{(3)}\lambda^{(j)}x_\zeta L^{(j)}W_{y'}+\lambda^{(3)}x_\zeta L^{(j)}B=0,
\end{aligned} \tag{3.11}$$

where $x_\zeta = 1/\zeta_x$, is the Jacobian of transformation and j = 1 to 4.

The vectors W and $W_{y'}$ are continuous across the wavefront $\zeta = 0$ and have their subscripts-0 valued whilst $W_{y'}$ and x_ζ are not continuous. On computing (3.11) at the rear side of the wavefront $\zeta = 0$ for $j = 1, 2, 4$, yields

$$u_\zeta = -\frac{1}{\rho_0 u_0} p_\zeta, \tag{3.12}$$

$$\rho_\zeta = \left(\frac{1}{C_0^2}\right) p_\zeta, \tag{3.13}$$

$$v_\zeta = \frac{\left(M_0^2 - 1\right)^{1/2}}{\rho_0 u_0} p_\zeta. \tag{3.14}$$

Now, on taking $j = 3$ in (3.11) and differentiate the produced equation w.r.t. ζ, then evaluate it at the rear side of wavefront $\zeta = 0$, yields

$$C_0^2 \left(M_0^2 - 1\right)^{1/2} p_{\zeta y'} + \rho_0 u_0 C_0^2 v_{\zeta y'} + \frac{n}{y'} \rho_0 C_0^2 u_0 v_\zeta = 0. \tag{3.15}$$

Using (3.14) in (3.15), we get

$$p_{\zeta y'} + \frac{n}{2y'} p_\zeta = 0. \tag{3.16}$$

On integrating (3.16) with respect to y', we have

$$p_\zeta = \left(\frac{y_0}{y'}\right)^{n/2} p_{\zeta 0}, \tag{3.17}$$

where $p_{\zeta 0} = \lim_{y' \to y_0} p_\zeta$, along $\zeta\,(x, y) = 0$.

As well, along $\zeta = constant$, we have

$$x_{y'} = 1/\lambda^{(3)}. \tag{3.18}$$

Differentiating (3.18) w.r.t. ζ and evaluate at the back side of $\zeta = 0$, yields

$$x_{\zeta y'} = -\frac{M_0^2\left((\Gamma+1) - 2\omega_2\rho_0^2\right)}{2\rho_0 C_0^2\left(M_0^2-1\right)^{1/2}\left(1-\omega_1\rho_0+\omega_2\rho_0^2\right)}\left(\frac{y_0}{y'}\right)^{n/2} p_{\zeta 0}. \tag{3.19}$$

Here, the equations (3.16) and (3.19) are required transport equations for the evolution of weak discontinuity.

3.4 Evolution of weak discontinuity

We will now discuss the evolution of weak discontinuity with the help of the above-derived transport equations (3.16) and (3.19). On integrating of (3.19) and using (3.17), we have

$$x_\zeta = 1 - \frac{M_0^2\left((\Gamma+1) - 2\omega_2\rho_0^2\right) y_0^{n/2} p_{\zeta 0}}{2\rho_0 C_0^2\left(M_0^2-1\right)^{1/2}\left(1-\omega_1\rho_0+\omega_2\rho_0^2\right)}\int_{y_0}^{y} t^{-n/2}\, dt, \tag{3.20}$$

where t is variable. $x_{\zeta 0} = x_\zeta \mid_{\zeta=0^-} = x_\zeta \mid_{\zeta=0^+} = 1$ and the boundary condition (3.10) is used in (3.20).

Suppose $y = Y(x)$ is the equation of the body contour with tangent at the tip of the body edge and parallel to the velocity of the streamline, we have

$$\frac{dy}{dx} = \frac{v}{u}. \tag{3.21}$$

On taking derivative of (3.21) with respect to ζ and computing behind $\zeta(x, y) = 0$,we obtain

$$v_{\zeta 0} = u_0 Y_0'', \tag{3.22}$$

where Y_0'' is known as curvature at the tip of the body.

From (3.14) and (3.22), (3.20) can be written in the form

$$x_\zeta = 1 - \frac{M_0^4\left((\Gamma+1) - 2\omega_2\rho_0^2\right) y_0^{n/2} Y_0''}{2\left(M_0^2-1\right)^{1/2}\left(1-\omega_1\rho_0+\omega_2\rho_0^2\right)} \int_{y_0}^{y} t^{-n/2}\, dt. \tag{3.23}$$

If the Jacobian x_ζ vanishes for some $y = y_t$, on the wavefront $\zeta = 0$, the characteristics of the family of neighboring $\zeta =$ constant must intersect on the wavefront $\zeta = 0$ and results in a discontinuity which is known as shock wave, occur in the solution vector W. If, we assume W_ζ is finite at $y = y_t$ as $x_\zeta = 0$, for then, just at the back of the wave front $\zeta = 0$, $W_x = \frac{W_\zeta}{x_\zeta}$ becomes infinite which is known as the steepening of the wavefront. The interpretation of (3.23) is discussed in detail in the next section for the values of $n = 0, 1$ and 2.

3.5 Results and discussion

Now, we will discuss the results as mentioned above, for the supersonic flow for three cases; first case ($n = 0$) is planar flow, second one is a cylindrically symmetric flow case ($n = 1$) and last one is spherically symmetric flow case ($n = 2$).

3.5.1 Planar flow

Steady two-dimensional planar flow is described in terms of two velocity components u and v as functions of two co-ordinates x and y by requiring that the component w vanish and that all quantities characterizing the flow are independent of z and t [1] (see Fig.3.1). For planar beak case, putting $n = 0$ in (3.23) and assume the body contour $y = Y_b(x)$ and sharp edge of the contour with vanishing small tangent

releasing the initial disturbance. Then (3.23) reduces in the following form

$$x_\zeta = 1 - \frac{Y_b''(0)}{\phi}\,(y - y_0)\,, \tag{3.24}$$

where,

$$\phi = \frac{2\,(M_0^2 - 1)\,(1 - \omega_1\rho_0 + \omega_2\rho_0^2)}{M_0^4\,((\Gamma + 1) - 2\omega_2\rho_0^2)}. \tag{3.25}$$

Here, $\phi > 0$ and $Y_b''(0)$ is the radius of curvature over the top of the body shape. As discussed previously, the vanishing of x_ζ describes the occurrence of a shock wave. We see that in (3.25), the Jacobian will vanish on ahead of wavefront for $y_0 < y$ only when $Y_b''(0) > 0$ with $Y_b''(0) > \phi$. Now, for $Y_b''(0) \leq \phi$, the Jacobian remains positive for $y_0 < y$ (finite) and there will be no shock created ahead of a wavefront. Thus, ϕ represents a critical level such that when this level is exceeded by $Y_b''(0)$, a discontinuity will form at a finite distance away from the body. It may be noticed that at $\zeta = 0$, v_x and v_ζ are related to each other by the relation $v_x = v_\zeta/x_\zeta$; therefore, it is inconsequential, and we get an expression for v_x and v_ζ at $\zeta = 0$. Since the physical explanation of v_x has slightly different, we shall choose to work in terms of that quantity for planar case, we have

$$v_x = \frac{C_0 M_0 Y_b''(0)}{1 - (Y_b''(0)/\phi)\,(y - y_0)}. \tag{3.26}$$

From the above equation, we see that when $Y_b''(0)$ is positive, and the modulus value of $Y_b''(0)$ is greater than ϕ, that is, $\mid Y_b''(0) \mid > \phi$, then the wave terminates into the shock and the corresponding equation of shock formation distance can be written as

$$y_t = y_0 + \frac{\phi}{Y_b''(0)}. \tag{3.27}$$

The equation (3.27) is derived from (3.26) when numerator remains finite, and its denominator is zero. Thus, the vanishing of x_ζ is clear from (3.27) which causes the steepening of waves into the shock wave. Also, for the case $Y_b''(0) \leq \phi$, the steepening of the velocity gradient does not happen while the wave is still compressive. Conversely, either v_ζ decreases along the wave head or remains constant if $Y_b''(0) < \phi$ or $Y_b''(0) = \phi$. From Fig.3.2, we can see that an increase in the value of upstream flow Mach number M_0 causes to decrease the shock formation distance y_t which means increasing values of upstream flow Mach number M_0 causes early shock formation. The parameter $\bar{b} = 0$ indicates the ideal gas and $k_p = 0$ is used for dust free gas. From Fig.3.2, it is clear that the presence of dust particles increases the shock formation distance that is the time of the occurrence of shock is accelerated by the dust particles. On exceeding the value of mass fraction of the dust particles, the shock formation distance increases in both ideal and non-ideal gas for planar flow case. Also, the presence of non-idealness in gas decreases the shock formation distance which is shown in Fig.3.2. In Fig.3.3, the curves represent the effect of volume fraction of dust particles in non-ideal dusty gas flow for planar case which insures that an increase in the value of volume fraction of dust particles causes to decrease the shock formation distance. It is obtained that the formation of shock will occur early on exceeding the value of the volume fraction of dust particles $\bar{Z}$, shown in Fig.3.3.

3.5.2 Cylindrically symmetric flow case

In cylindrical flow case, a two-dimensional flow in which all quantities depend only on the distance from the axis and velocity is directed away from (or toward) the axis (see Fig. 3.4).

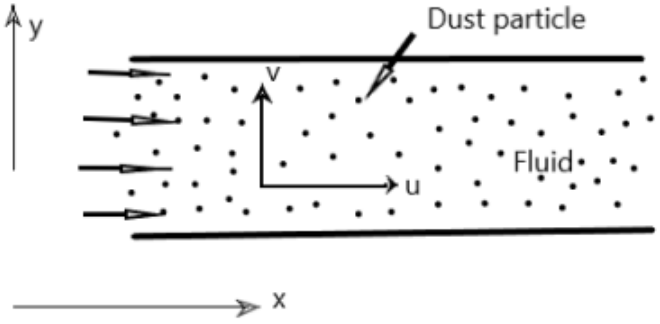

FIGURE 3.1: Two-dimensional geometry for planar case

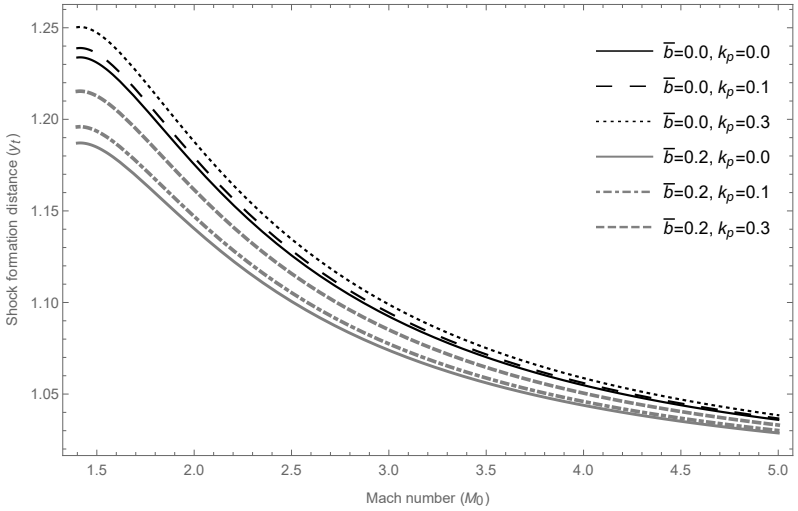

FIGURE 3.2: The effect of dust particles on the shock formation distance in ideal and non-ideal planar gas flow with $\gamma = 1.67$, $\beta = 0.8$, $\bar{Z} = 0.01$ and $Y_b''(0) = 1$.

In the present case, we consider $y = Y_t(x)$, with sharp edged entry releasing the initial disturbance which runs inward and outward both along characteristics lines. For $y_0 < y$, the behavior is similar as observed in planar flow which is mentioned above. Now putting $n = 1$ in (3.23), we have

$$x_\zeta = 1 - Y_t''(0) J_0 \left(y^{1/2} - y_0^{1/2} \right), \tag{3.28}$$

where

$$J_0 = \frac{((\Gamma + 1) - 2\omega_2 \rho_0^2)\, y_0^{1/2} M_0^4}{(M_0^2 - 1)\,(1 - \omega_1 \rho_0 + \omega_2 \rho_0^2)}.$$

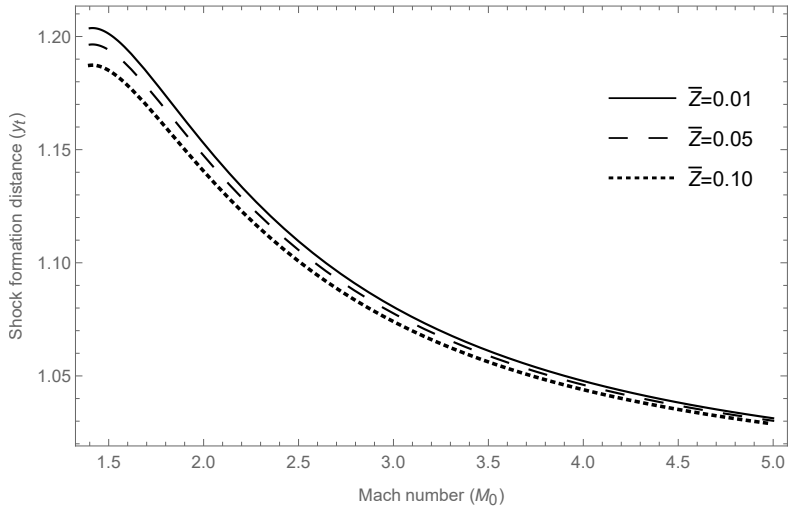

FIGURE 3.3: The effect of volume fraction of dust particles on the shock formation distance in non-ideal dusty planar gas flow with $\gamma = 1.67$, $\beta = 0.8$, and $Y_b''(0) = 1$.

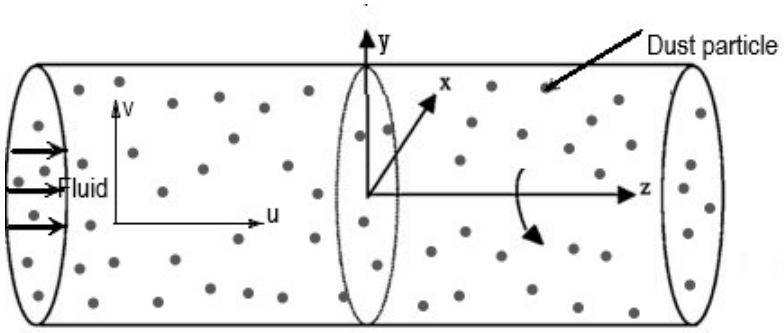

FIGURE 3.4: Two-dimensional geometry for cylindrical case

In view of (3.28), we observe that for $y_0 < y$, the right hand side of (3.28) lies between zero and one. There by, the Jacobian x_ζ will vanish, which leads to the occurrence of a shock wave, provided $Y_t''(0) > 0$ and $Y_t''(0) > J_0^{-1}$. If $Y_t''(0) \leq J_0^{-1}$, $x_\zeta > 0$, there will not occur any shock wave on the leading wavefront. Hence, one can observe that the formation of a shock will take place only when $Y_s''(0) > J_0^{-1}$, so for the ordinate $y = y_t$, the equation for the shock formation distance when the first shock occurs can be written as

$$y_t^{1/2} = y_0^{1/2} + \frac{1}{J_o Y_t''(0)}. \tag{3.29}$$

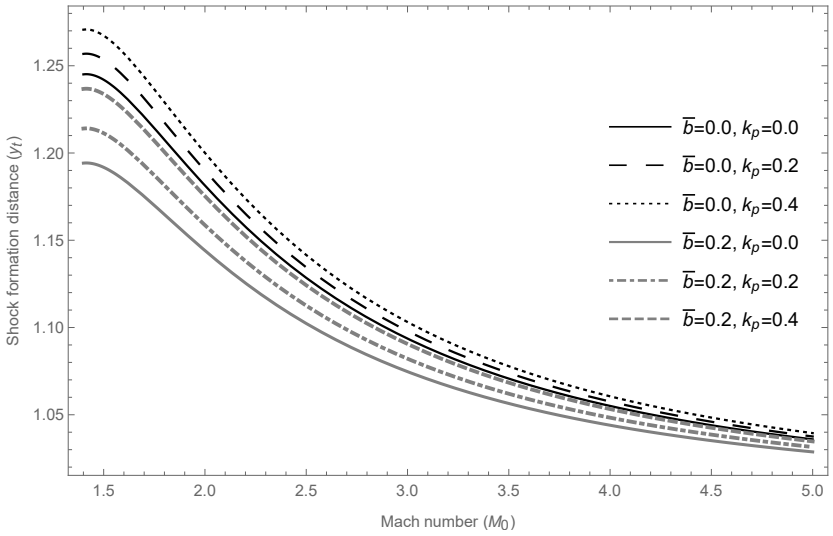

FIGURE 3.5: The effect of dust particles on the shock formation distance in ideal and non-ideal cylindrically symmetric gas flow with $\gamma = 1.67$, $\beta = 0.8$, $\bar{Z} = 0.01$ and $Y_b''(0) = 1$.

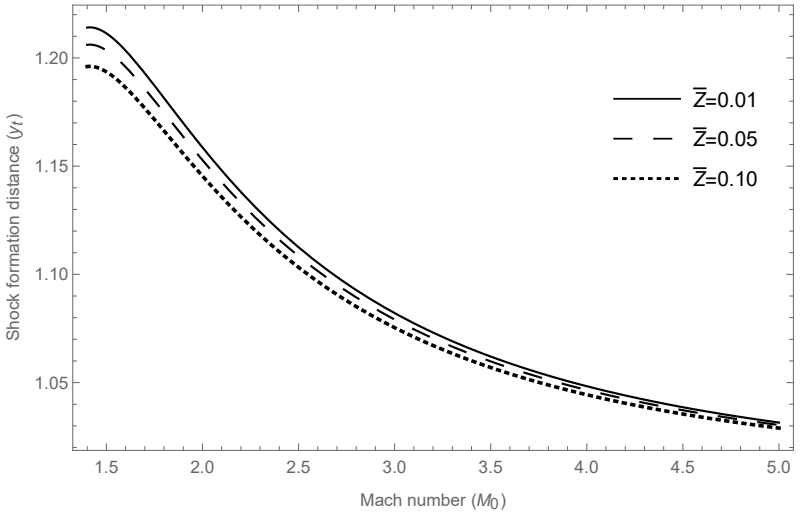

FIGURE 3.6: The effect of volume fraction of dust particles on the shock formation distance in non-ideal dusty cylindrically symmetric gas flow with $\gamma = 1.67$, $\beta = 0.8$, and $Y_b''(0) = 1$.

For cylindrically symmetric flow case, the solution curves corresponding to the equation (3.29) is represented in Figs.3.5 and 3.6. From Fig.3.5, it is observed that the presence of dust particles accelerates the shock formation distance y_t in ideal and van der Waals gas flows that is the value of y_t increases on increasing the value of k_p, but it decreases on increasing the value of upstream flow Mach number M_0 and

non-ideal parameter $\bar{b}$. Fig.3.6 shows that the shock formation distance decreases with an increase in the value of volume fraction of dust particles in van der Waals gas.

3.5.3 Spherically symmetric flow

In spherical flow case, flow occurs when all quantities depend only on the distance from one point, chosen as the origin, in addition to the time, and if the velocity is directed away from the (or towards) this point (see Fig.3.7).

For spherically symmetric flow of gas, for $0 < y_0 < y$, similar trend is seen as in cylindrically symmetric flow. Now putting $n = 2$ into (3.23), we obtain

$$x_\zeta = 1 - K_0 Y_t'' log\left(\frac{y}{y_0}\right), \tag{3.30}$$

where

$$K_0 = \frac{M_0^4\left((\Gamma+1) - 2\omega_2\rho_0^2\right)y_0}{2\left(M_0^2-1\right)\left(1-\omega_1\rho_0+\omega_2\rho_0^2\right)}.$$

As previously discussed, the Jacobian x_ζ will vanish, which leads to the occurrence of a shock wave, provided $Y_t''(0) > 0$ and $Y_t''(0) > K_0^{-1}$. Then, the equation for the shock formation distance can be written as

$$y_t = y_0 e^{\frac{1}{K_0 Y''}}. \tag{3.31}$$

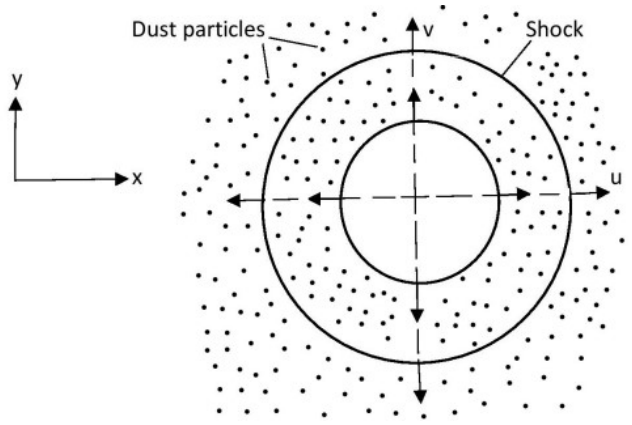

FIGURE 3.7: Two-dimensional geometry for spherically symmetric case

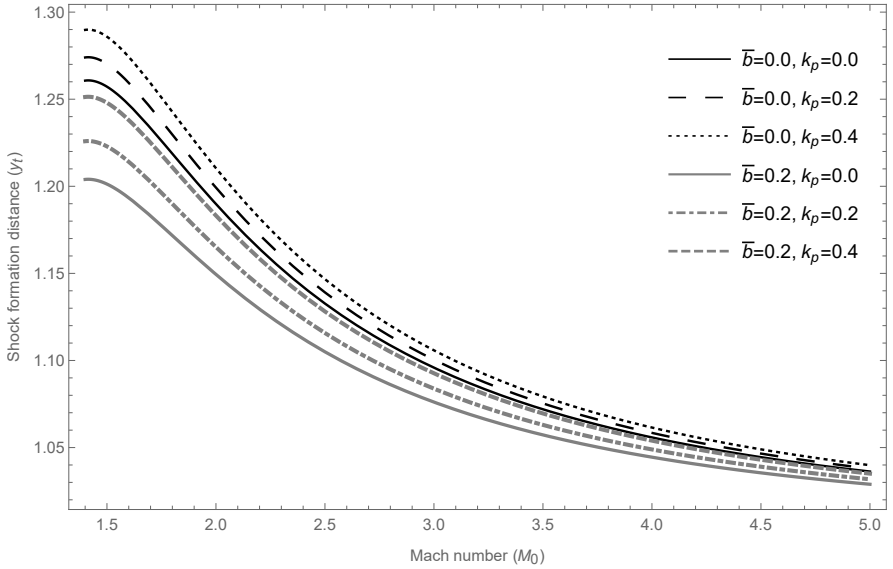

FIGURE 3.8: The effect of dust particles on the shock formation distance in ideal and non-ideal spherically symmetric gas flow with $\gamma = 1.67$, $\beta = 0.8$, $\bar{Z} = 0.01$ and $Y_b''(0) = 1$.

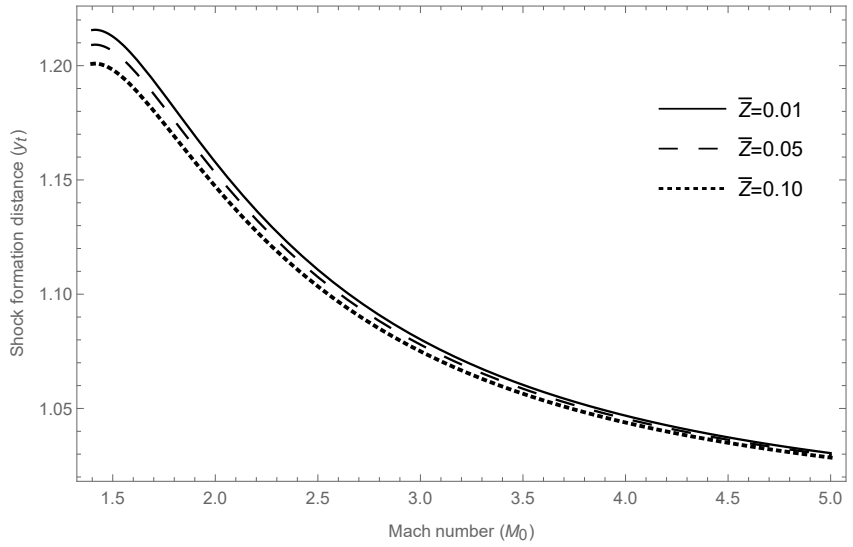

FIGURE 3.9: The effect of volume fraction of dust particles on the shock formation distance in non-ideal dusty spherically symmetric gas flow with $\gamma = 1.67$, $\beta = 0.8$, and $Y_b''(0) = 1$.

In this case, the solution curves corresponding to (3.31), is represented in Figs.3.8 and 3.9, which shows the similar phenomena of shock formation as in cylindrically symmetric case. From Fig.3.8, it is clear that an increase in the value of non-ideal parameter and Mach number decreases the value of y_t as in cylindrically symmetric case. From Fig.3.9, it is also observed that y_t decreases with an increase in the value of volume fraction of dust particles for spherically symmetric flow case which is same as cylindrically symmetric case.

In Fig.3.10, we analyze the difference of the shock formation for planar flow case ($n = 0$), cylindrically symmetric case ($n = 1$) and spherically symmetric flow case ($n = 2$) in non-ideal dusty gas dynamics. We observed that an increase in the value of M_0 have effect to decrease the value of y_t for all cases together with fixed value of all parameters of non-ideal dusty gas flow. From Fig.3.10, it is clear that in case of planar flow, shock will occur early in comparison to other two cases. In this study, it is also analyzed that the specific heat ratio γ present in the expression for shock formation distance influences the time of occurrence of shock wave which is shown in

Fig.3.11. From Fig.3.11, it is noticeable that the shock formation distance decreases with an increase in the value of specific heat ratio together with Mach number in van der Waals gas flow with dust particles.

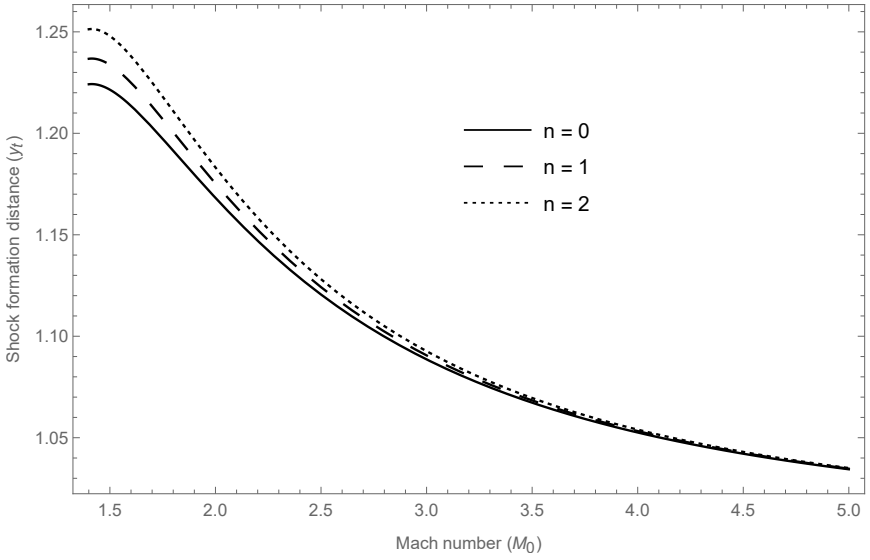

FIGURE 3.10: Comparison of planar, cylindrically symmetric and spherically symmetric cases for the shock formation distance in non-ideal dusty gas flow with $\gamma = 1.67$, $\beta = 0.8$, $\bar{Z} = 0.01$ and $Y_b''(0) = 1$.

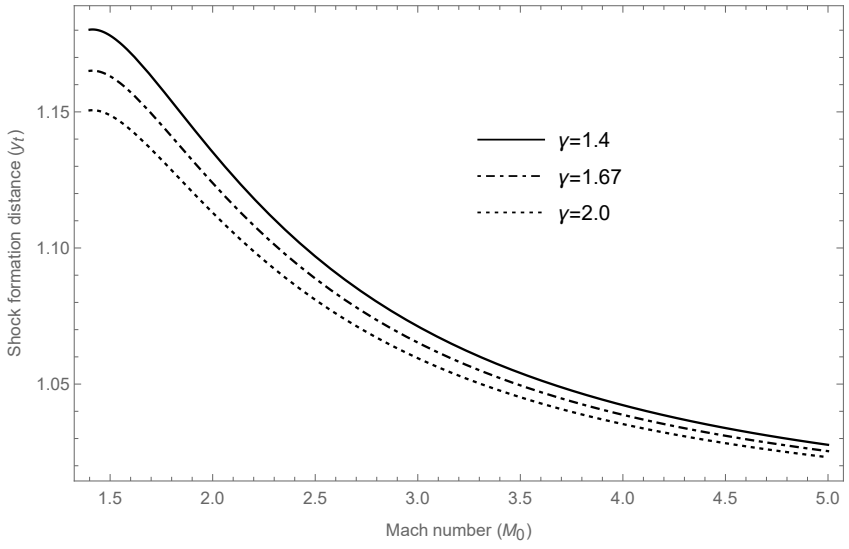

FIGURE 3.11: The effect of specific heat ratio on the shock formation distance in non-ideal dusty gas flow with $\gamma = 1.67$, $\beta = 0.8$, $\bar{Z} = 0.01$ and $Y_b''(0) = 1$.

3.6 Conclusions

In the present work, we have investigated the formation of shock wave in 2-D steady inviscid supersonic non-ideal dusty gas flow for "planar, cylindrically symmetric and spherically symmetric cases" using method of wavefront analysis. It is obtained that the system of the governing equations describing the composition of van der Waals gas and dust particles is hyperbolic system. Furthermore, we derived the transport equations for the evolution of discontinuities which insures the condition that there will not evolve any shock on the wavefront. Also, the relation for the shock formation distance is derived and it is obtained that the shock formation distance is a decreasing function of M_0. It is analyzed that the presence of dust particles in van der Waals gas flow increases the shock formation distance and an increase in the value of Mach number accelerate the process of shock formation. It is also observed that due to the impact of non-idealness in dusty gas flow, shock occurs earlier as compared to dusty gas that is an increase in the value of non-ideal parameter causes to decrease the value of y_t in dusty gas. The impact of volume fraction of dust particle and specific heat ratio on the occurrence of the shock is examined and it is obtained that an increase in the amount of dust particles in the fluid causes an early shock formation. Also, the phenomena of shock formation in the composition of van der Waals gas and dust particles is analyzed for "planar, cylindrically symmetric and spherically symmetric cases" which provide similar behavior of shock formation. It is observed that in planar case, there is an early shock formation as compared to non-planar cases on increasing the value of M_0. In the absence of van der Waals gas parameter ($\bar{b} = 0$), the results obtained in this study is in close agreement with the results reported in the literature [83].

****